An analysis of the dynamical frictional unilateral contact problems of beams and plates on Hetény's foundation

L. ASCIONE, G. BILOTTI*

ABSTRACT: In this paper the dynamical frictional contact problem of an elastic plate resting on a Hetényi's foundation is analyzed from a computational point of view. The friction law assumed there is based on a regularization of Coulomb's classical law.
The analysis concerns some one-dimensional models of beams and axisymmetric circular plates.
The numerical investigation is carried out by a finite element approach and the time integration of the discretized dynamical is obtained using a semi-implicit method.
The numerical results obtained show how the main parameters involved in the analysis influence the dynamical solution.

1. Introduction

It is often found in practical applications that the area of contact between soil and foundation structure is reduced either because of the particular loading conditions acting or because of the relative stiffness of the soil-structure involved. Since it is impossible to hypohesize perfect bonding at the interface in these particular cases, it is obvious that the problem of unilateral contact is of considerable importance.

Although this subject has been extensively researched, particularly in the field of statics [GLADWELL 1980; DUVAUT e LIONS, 1980], it would appear that the dynamic problem involving unilateral constraints has been somewhat neglected [PANAGIOTOPOULOS, TASLADIS, 1980; MITSOPOULOU, 1983; TOSCANO, 1983; ASCIONE *et al.*, 1984].

Dynamic problems do indeed present far greater difficulties than static ones. However, some advantages are to be gained by using simplified soil models which enable the more significant mechanical features to be analyzed fairly easily.

A detailed description of such models is given in [SELVADURAI, 1979].

Examples of how this type of analysis can be applied to Winckler's model are given in [ASCIONE *et al.*, 1984].

However, it is possible to obtain more realistic results by using the so-called *two-parameter models*, which are characterized by two indipendent elastic constants.

Hetényi's model, in particular, in view of technical applications, seems to be very useful. As well know it simulates the soil by means of bilateral springs connected by an elastic plate.

In previous papers [ASCIONE *et al.*, 1986; ASCIONE, BILOTTI, 1989], we analysed the frictionless dynamical contact problem relative to some one-dimensional models of beams and axisymmetric circular plates in unilateral contact with a Hetényi's foundation.

In the present paper this analysis also covers the effect of frictional stresses at the interface between the structure and soil. The law of friction under consideration can be seen as a regularization of Coulomb's classical law. Previous application of the same law in the statical field can be found in [ASCIONE, BRUNO, 1984; BILOTTI, OLIVITO, 1986].

In particular we will limit ourselves to consider only one-dimensional models of beams and axisymmetric circular plates. The problem will be formulated and analysed from a numerical point of view.

The mathematical aspects will be discussed in a future paper. For the present the numerical results, that we have obtained by means of a finite element technique, show how the most important parameters involved in the analysis influence the solution.

2. Formulation of the problem

With reference to Fig. 1, let us consider the dynamical problem of an elastic plate π_p resting on a Hetényi's foundation π_s. Let us suppose the contact to be unilateral and with friction.

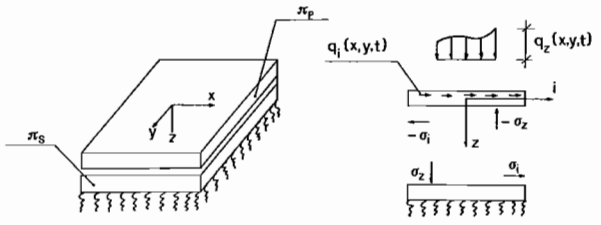

Fig. 1

*Prof. Ing. Luigi Ascione, Dott. Ing. Giancarlo Bilotti - Istituto di Ingegneria Civile - Università di Salerno.

Furthermore let us suppose that the plate π_p can undergo stretching deformation while the plate π_s is inextensible.

Let:

Ω	be a region of R^2 with sufficiently smooth boundary;
$\mathbf{u}_p = (u_p, v_p, w_p)$	the diplacements of the plate π_p;
w_s	the transverse deflection of the plate π_s;
$\sigma = (\sigma_x, \sigma_y, \sigma_z)$	the interaction stresses between plate and foundation;
$\mathbf{q} = (q_x, q_y, q_z)$	the external loads acting on the plate;
ρ_i (>0)	the mass density of π_i $(i = p, s)$;
D_i (>0)	the flexural stiffness of π_i $(i = p, s)$;
ν_i $(0<\nu_i<1/2)$	the Poisson's ratio of π_i $(i = p, s)$;
C_p (>0)	the extensional stiffnes of π_p;
k (>0)	the elastic constant of the vertical springs in Hetényi's foundation;
$(\cdot)^{\cdot} = \dfrac{\partial(\cdot)}{\partial t}$	the time derivative of $(\cdot)$ $(t \in [0, T], T>0)$;
$L^2(\Omega)$	the space of the square summable functions on Ω;
$H^n(\Omega)$ $(n \geqslant 1)$	the Sobolev space of order n on Ω;
$\mathbf{V}_p = H^1(\Omega) \times H^1(\Omega) \times H^2(\Omega)$	the space of the admissible displacements of π_p;
$V_s = H^2(\Omega)$	the space of the admissible displacements of π_s;
$\langle \cdot, \cdot \rangle$	the duality pairing between dual space;
$\lvert \cdot \rvert$	the norm symbol in $L^2(\Omega)$;
$\lVert \cdot \rVert_V$	the norm symbol on the Hilbert space V;
$\mathbf{A}_i : \mathbf{V}_i \to \mathbf{V}_i'$ $(i = p, s)$	the linear operator associate with the symmetric bilinear form $a_i(\mathbf{u}_i, \delta\mathbf{u}_i)$ defined on the space $\mathbf{V}_i$ as follows:

$$
\begin{aligned}
\mathbf{a}_i(\mathbf{u}_i, \delta\mathbf{u}_i) = D_i \int_\Omega \Bigg[& \frac{\partial^2 w_i}{\partial x^2} \frac{\partial^2 \delta w_i}{\partial x^2} + 2(1-\nu_i) \frac{\partial^2 w_i}{\partial x\, \partial y} \frac{\partial^2 \delta w_i}{\partial x\, \partial y} + \\
& + \nu_i \frac{\partial^2 w_i}{\partial x^2} \frac{\partial^2 \delta w_i}{\partial y^2} + \nu_i \frac{\partial^2 w_i}{\partial y^2} \frac{\partial^2 \delta w_i}{\partial x^2} + \frac{\partial^2 w_i}{\partial y^2} \frac{\partial^2 \delta w_i}{\partial y^2} \Bigg] d\Omega + \\
+ \delta_{ip} C_p \int_\Omega \Bigg[& \frac{\partial u_p}{\partial x} \frac{\partial \delta u_p}{\partial x} + \frac{\partial v_p}{\partial y} \frac{\partial\, \delta v_p}{\partial y} + \nu_p \left(\frac{\partial u_p}{\partial x} \frac{\partial\, \delta v_p}{\partial y} + \frac{\partial\, \delta u_p}{\partial x} \frac{\partial v_p}{\partial y} \right) + \\
& + \frac{1-\nu_p}{2} \left(\frac{\partial u_p}{\partial y} + \frac{\partial v_p}{\partial x} \right) \left(\frac{\partial\, \delta u_p}{\partial y} + \frac{\partial\, \delta v_p}{\partial x} \right) \Bigg] d\Omega
\end{aligned}
\tag{2.1}
$$

δ_{ip} being the kronecker symbol.

It is well known [DUVAUT, LIONS, 1980] that the following result holds:

$$\forall\, b>0,\ \exists\, b_p,\ b_s>0:$$

$$a_p(\mathbf{u}, \mathbf{u}) + b_p \lvert \mathbf{u} \rvert^2 \geqslant b \lVert \mathbf{u} \rVert^2_{\mathbf{v}_p}, \quad \forall \mathbf{u} \in \mathbf{V}_p, \tag{2.2a}$$

$$\mathbf{a}_s(w, w) + b_s \lvert w \rvert^2 \geqslant b \lVert w \rVert^2_{V_s}, \quad \forall w \in \mathbf{V}_s. \tag{2.2b}$$

With refecence to the friction law, we assume that at the interface between structure and foundation a tangential surface force $\tau = (\sigma_x, \sigma_y, 0)$ is active which is related to the horizontal velocities by means of the relations:

$$\tau = \varepsilon_1 \dot{\delta} + (\varepsilon_2 - \varepsilon_1)\, (\lvert \dot{\delta} \rvert - f\sigma_z/\varepsilon_1)^+ \frac{\dot{\delta}}{\lvert \dot{\delta} \rvert} \tag{2.3}$$

where:

ε_1, ε_2 - are two assigned positive constants,

$\delta = (\delta_x, \delta_y, 0)$ - is the horizontal component of the displacement corresponding to a generic point belonging to the plate surface in contact with the foundation:

$$\delta_x = u_p - \frac{\partial w_p}{\partial x} \frac{h}{2}, \tag{2.4a}$$

$$\delta_y = v_p - \frac{\partial w_p}{\partial y} \frac{h}{2}, \tag{2.4b}$$

h being the plate thickness,

f (> 0) is the coefficient of friction,

$(\cdot)^+$ is the positive part of $(\cdot)$,

$|\dot{\delta}| = [(\dot{\delta}_x)^2 + (\dot{\delta}_y)^2]^{1/2}$.

The relation (2.3) is semplified for a monodimensional case in Fig. 2. It is easy to recognize that for $\varepsilon_1 \to \infty$ and $\varepsilon_2 \to 0$ the friction law (2.3) approximates the classical law of dynamical friction proposed by Coulomb.

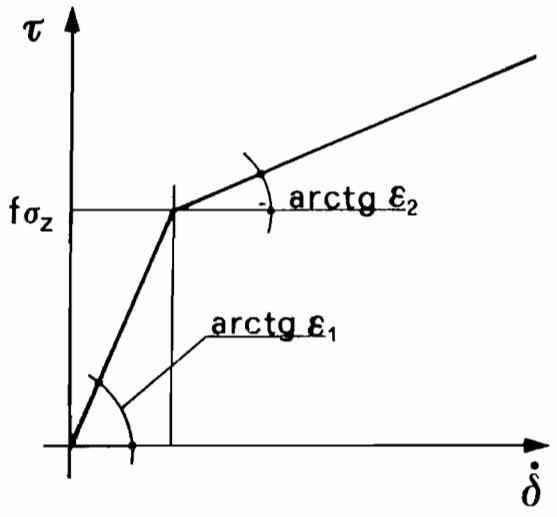

Fig. 2

After these preliminaries the dynamical problem previously examined can be formulated as follows:

Problem P

Let $\mathbf{q}$ (x, y, t) be element of L^∞ (0, T; $\mathbf{V}_p'$). Find $\mathbf{u}_p$ (x, y, t) $\in \mathbf{L}^\infty$ (0, T; $\mathbf{V}_p$), $w_s \in L^\infty$ (0, T; V_s) and $\sigma_z \in L^\infty$(0,T; V_s') satisfying the following equations:

$$\langle \rho\, \ddot{\mathbf{u}}_p + \mathbf{A}_p\, \mathbf{u}_p - \mathbf{q} + \sigma,\ \delta\mathbf{u}_p \rangle +$$

$$- \left\langle \frac{h}{2}\, \sigma_x,\ \frac{\partial \delta w_p}{\partial x} \right\rangle - \left\langle \frac{h}{2}\, \sigma_y,\ \frac{\partial \delta w_p}{\partial y} \right\rangle = 0 \quad (2.6a)$$

$$\langle \rho_s\, \ddot{w}_s + A_s\, w_s + k\, w_s - \sigma_z,\ \delta w_s \rangle = 0, \quad (2.6b)$$

$$w_s - w_p \geqslant 0, \quad (2.6c)$$

$$\sigma_z \geqslant 0, \quad (2.6d)$$

$$\langle \sigma_z,\ w_s - w_p \rangle = 0, \quad (2.6e)$$

$$\forall\ \delta\mathbf{u}_p \in \mathbf{V}_p \text{ and } \forall\ \delta w_s \in V_s.$$

We recall that in eq. (2.6a) the stresses σ_x and σ_y are related to the unknown displacements by means of the relations (2.3) and (2.4).

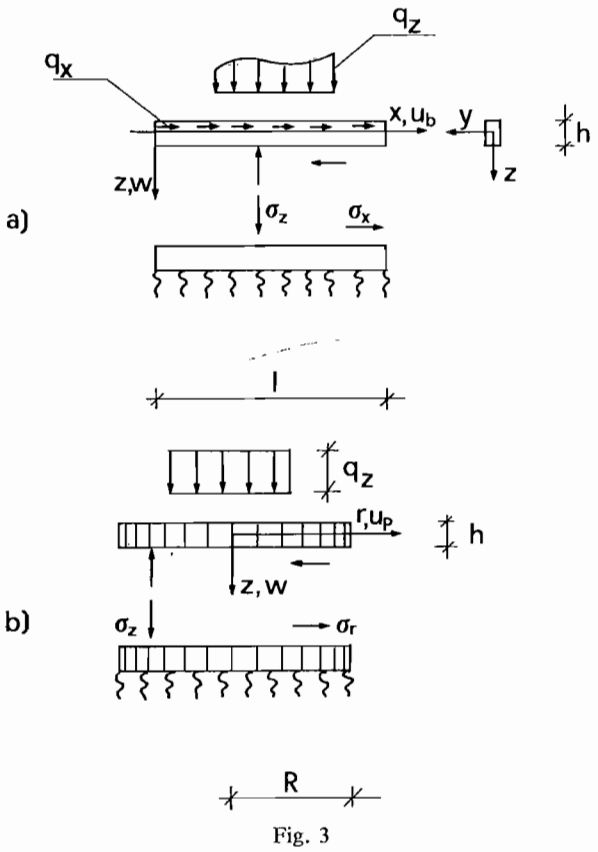

Fig. 3

3. Applications

In this section we will examine two applications of Problem P relative to the one-dimensional models shown in Fig. 3a and 3b.

The first one is a beam of a rectangular cross section and the second is an axisymmetric circular plate.

In order to overcome the mathematical difficulties related with the presence of the inequalities (2.6c) and (2.6d), it is helpful to refer to an auxiliary problem obtained from Problem P by modifying the contact conditions. More precisely, following a procedure still applied in Ascione e Bilotti [1989], we will suppose that the plate π_p can present lateral deflections which are greater than the corrisponding deflections in the foundation (Fig. 4).

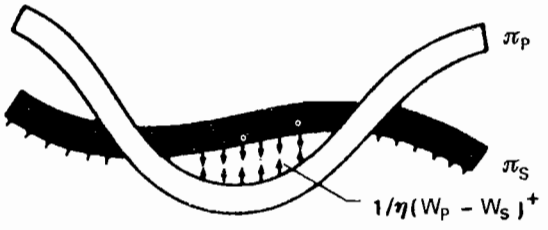

Fig. 4

Nevertheless, where the condition $(w_p - w_s) > 0$ is verified, some springs of stiffness $1/\eta$ are active and they suppose the interpenetration of the two bodies. It is easy to conjecture that when $\eta \to 0$, i.e. when the spring stiffness increases indefinitely, the auxiliary problem approximates the previous one.

From a mathematical point of view the auxiliary problem can be formulated as follows:

Problem A

Let $\mathbf{q}$ be as in Problem P. Find $\mathbf{u}_p \in L^\infty(0, T; \mathbf{V}_p)$ and $w_s \in L^\infty(0, T; V_s)$ such that:

$$\langle \rho_p \ddot{\mathbf{u}}_p, \delta\mathbf{u}_p \rangle + \langle \mathbf{A}_p \mathbf{u}_p, \delta\mathbf{u}_p \rangle + \langle \sigma_s \ddot{w}_s, \delta w_s \rangle + \langle A_s w_s, \delta w_s \rangle + \langle k w_s, \delta w_s \rangle + \langle \frac{1}{\eta} (w_p - w_s)^+, \delta w_p - \delta w_s \rangle - \langle \mathbf{q}, \delta\mathbf{u}_p \rangle + (3.1)$$
$$- \langle \frac{h}{2} \sigma_x, \frac{\partial \delta w_p}{\partial x} \rangle - \langle \frac{h}{2} \sigma_y, \frac{\partial \delta w_p}{\partial y} \rangle + \langle \tau, \delta\mathbf{u}_p \rangle = 0$$
$$\forall\, \delta\mathbf{u}_p \in \mathbf{V}_p \text{ and } \forall\, \delta w_s \in V_s .$$

We now give the expression of all the terms in eq. (3.1) for the two cases examined in Fig. 3. By the prime we will denote the derivative respect to the abscissa along the beam axis or along the plate radius.

Beam	Circular Plate
$\langle \mathbf{A}_p \mathbf{u}_p, \delta\mathbf{u}_p \rangle = D_b \int_0^\ell w_b'' \, \delta w_b'' \, dx + C_b \int_0^\ell u_b' \, \delta u_b' \, dx$	$\langle \mathbf{A}_p \mathbf{u}_p, \delta\mathbf{u}_p \rangle = 2\pi D_p \int_0^R [r\, w_p'' \, \delta w_p'' + \frac{1}{r} w_p' \, \delta w_p' + \nu_p (w_p'' \, \delta w_p' + w_p' \, \delta w_p'')] \, dr + 2\pi C_p \int_0^R \left[\frac{1}{r} u_p \, \delta u_p + \nu_p (u_p' \, \delta u_p + u_p \, \delta u_p') + r\, u_p' \, \delta u_p' \right] dr$ (3.2)
$\langle A_s w_s, \delta w_s \rangle = D_s \int_0^\ell w_s'' \, \delta w_s'' \, dx$	$\langle A_s w_s, \delta w_s \rangle = 2\pi D_s \int_0^R [r\, w_s'' \, \delta w_s'' + \frac{1}{r} w_s' \, \delta w_s' + \nu_s (w_s'' \, \delta w_s' + w_s' \, \delta w_s'')] \, dr$ (3.3)
$\langle \rho_p \ddot{\mathbf{u}}_p, \delta\mathbf{u}_p \rangle = \int_0^R \rho_b [\ddot{u}_b \, \delta u_b + \ddot{w}_b \delta w_b] \, dx$	$\langle \rho_p \ddot{\mathbf{u}}_p, \delta\mathbf{u}_p \rangle = 2\pi \rho_p \int_0^R [\ddot{u}_p \, \delta u_p + \ddot{w}_p \, \delta w_p] \, r \, dr$ (3.4)
$\langle \rho_s \ddot{w}_s, \delta w_s \rangle = \int_0^\ell \rho_s \ddot{w}_s \, \delta w_s \, dx$	$\langle \rho_s \ddot{w}_s, \delta w_s \rangle = 2\pi \rho_s \int_0^R \ddot{w}_s \, \delta w_s \, r \, dr$ (3.5)
$\langle k w_s, \delta w_s \rangle = k \int_0^\ell w_s \, \delta w_s \, dx$	$\langle k w_s, \delta w_s \rangle = 2\pi k \int_0^R w_s \, \delta w_s \, r \, dr$ (3.6)
$\langle 1/\eta \, (w_p - w_s)^+, \delta w_p - \delta w_s \rangle = 1/\eta \int_0^\ell (w_b - w_s)^+ (\delta w_b - \delta w_s) \, dx$	$\langle 1/\eta \, (w_p - w_s)^+, \delta w_p - \delta w_s \rangle = 2\pi/\eta \int_0^R (w_p - w_s)^+ (\delta w_p - \delta w_s) \, r \, dr$ (3.7)
$\langle \frac{h}{2} \sigma_x, \delta w_p' \rangle = \int_0^\ell \frac{h}{2} \sigma_x \, \delta w_b' \, dx$	$\langle \frac{h}{2} \sigma_r, \delta w_p' \rangle = 2\pi \int_0^R \frac{h}{2} \sigma_r \, \delta w_p' \, r \, dr$ (3.8)
$\langle \tau, \delta\mathbf{u}_p \rangle = \int_0^\ell \sigma_x \, \delta u_b \, dx$	$\langle \tau, \delta\mathbf{u}_p \rangle = 2\pi \int_0^R \sigma_r \, \delta u_p \, r \, dr$ (3.9)

where

$$\sigma_\chi = \varepsilon_1 \bar{u}_b + (\varepsilon_2 - \varepsilon_1)\left(\left|\dot{u}_b + \frac{h}{2}\dot{w}_b'\right| + \right.$$
$$\left. - \dot{u}_0\right)^+ \frac{\bar{u}_b}{|\bar{u}_b|}$$

being:

$$\bar{u}_b = \dot{u}_b + \frac{h}{2}\dot{w}_b', \quad \dot{u}_0 = \frac{1}{\varepsilon_1}\frac{(w_b - w_s)^+}{\eta}.$$

where

$$\sigma_r = \varepsilon_1 \bar{u}_p + (\varepsilon_2 - \varepsilon_1)\left(\left|\dot{u}_p + \frac{h}{2}\dot{w}_p'\right| + \right.$$
$$\left. - \dot{u}_0\right)^+ \frac{\bar{u}_p}{|\bar{u}_p|} \qquad (3.10)$$

being:

$$\bar{u}_p = \dot{u}_p + \frac{h}{2}\dot{w}_p', \quad \dot{u}_0 = \frac{1}{\varepsilon_1}\frac{(w_p - w_s)^+}{\eta}. \qquad (3.11)$$

4. Finite element approximation

With reference to Fig. 5

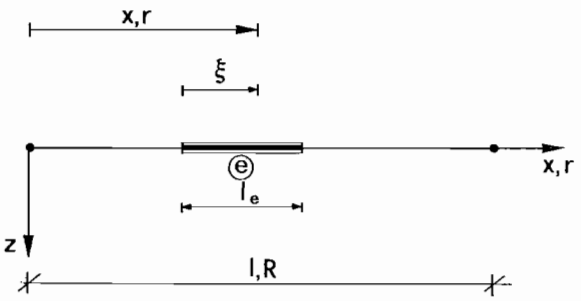

Fig. 5

let us consider a division of the interval [0, R] into N_e finite elements of egual length, over which the unknown functions u_p (axial diplacement) and w_i (lateral deflection of π_i, i = p, s) are interpolated as follows:

$$u_p^{(e)}(\xi, t) = \sum_\alpha u_\alpha^{(e)}(t)\, f_{u\alpha}^{(e)}(\xi) = \mathbf{F}_u^T\, \mathbf{u}^{(e)} \qquad (4.1a)$$

$$w_i^{(e)}(\xi, t) = \sum_\beta w_{i\beta}^{(e)}(t)\, f_{w\beta}^{(e)}(\xi) = \mathbf{F}_w^T\, \mathbf{w}_i^{(e)} \qquad (4.1b)$$

where $u_\alpha^{(e)}$ and $w_{i\beta}^{(e)}$ (t) are the nodal values of $\mathbf{u}_p^{(e)}$, $\mathbf{w}_i^{(e)}$ and the functions $f_{u\alpha}^{(e)}$ $f_{w\beta}^{(e)}$ represent the local interpolants [12].

Given eqs. (4.1a) and (4.1b) we can reexpress the terms of eqs. (3.2)-(3.9) in the following form:

$$\langle \mathbf{A}_p\, \mathbf{u}_p, \delta\mathbf{u}_p\rangle = \sum_e \delta\mathbf{v}_p^{(e)T}\, \mathbf{K}_p^{(e)}\, \mathbf{v}_p^{(e)}, \qquad (4.2)$$

where:

$$\mathbf{v}_p^{(e)} = \begin{bmatrix} \mathbf{u}_p^{(e)} \\ \mathbf{w}_p^{(e)} \end{bmatrix}, \quad \mathbf{K}_p^{(e)} = \left[\begin{array}{c|c} \mathbf{K}_u^{(e)} & \mathbf{0} \\ \hline \mathbf{0} & \mathbf{K}_w^{(e)} \end{array}\right], \qquad (4.3)$$

being:

$$\mathbf{K}_u^{(e)} = C_b \int_0^{\ell e} \mathbf{F}_u'\, \mathbf{F}_u'^T\, d\xi,$$

$$\mathbf{K}_w^{(e)} = D_b \int_0^R \mathbf{F}_w''\, \mathbf{F}_w''^T\, d\xi;$$

$$\mathbf{K}_u^{(e)} = 2\pi C_p \left\{ \int_0^{\ell e} \left[\frac{1}{r}\mathbf{F}_u\, \mathbf{F}_u^T + \nu_p\,(\mathbf{F}_u\, \mathbf{F}_u'^T + \right.\right.$$
$$\left.\left. + \mathbf{F}_u'\, \mathbf{F}_u^T) + r\, \mathbf{F}_u'\, \mathbf{F}_u'^T\right] d\xi\right\}, \qquad (4.4)$$

$$\mathbf{K}_w^{(e)} = 2\pi D_p \left\{ \int_0^{\ell e} \left[r\, \mathbf{F}_w''\, \mathbf{F}_w''^T + \frac{1}{r}\, \mathbf{F}_w'\, \mathbf{F}_w^T + \right.\right.$$
$$\left.\left. + \nu_p\,(\mathbf{F}_w''\, \mathbf{F}_w'^T + \mathbf{F}_w'\, \mathbf{F}_w^T)\right] d\xi\right\}; \qquad (4.5)$$

$$\langle \mathbf{A}_s\, w_s, \delta w_s\rangle = \sum_e \delta\mathbf{w}_s^{(e)T}\, \mathbf{K}_s^{(e)}\, \mathbf{w}_s^{(e)}, \qquad (4.6)$$

where the matrix $\mathbf{K}_s^{(e)}$ is obtained from eq. (4.5) by substituting D_s and ν_s to D_i and ν_i (i = b,p);

$$\langle \rho_p\, \ddot{u}_p, \delta\mathbf{u}_p\rangle = \sum_e \delta\mathbf{v}_e^{(e)T}\, \mathbf{M}^{(e)}\, \ddot{\mathbf{v}}_p^{(e)}, \qquad (4.7)$$

where:

$$\mathbf{M}^{(e)} = \left[\begin{array}{c|c} \mathbf{M}_u^{(e)} & \mathbf{0} \\ \hline \mathbf{0} & \mathbf{M}_w^{(e)} \end{array}\right], \tag{4.8}$$

being:

$$\mathbf{M}_u^{(e)} = \rho_b \int_0^{\ell e} \mathbf{F}_u \, \mathbf{F}_u^T \, d\xi, \qquad \mathbf{M}_u^{(e)} = 2\pi\rho_p \int_0^{\ell e} \mathbf{F}_u \, \mathbf{F}_u^T \, t \, d\xi, \tag{4.9}$$

$$\mathbf{M}_w^{(e)} = \rho_b \int_0^{\ell e} \mathbf{F}_w \, \mathbf{F}_w^T \, d\xi; \qquad \mathbf{M}_w^{(e)} = 2\pi\rho_p \int_0^{\ell e} \mathbf{F}_w \, \mathbf{F}_w^T \, r \, d\xi; \tag{4.10}$$

$$\langle \rho_s \ddot{w}_s, \, \delta w_s \rangle = \sum_e \delta \mathbf{w}_s^{(e)T} \, \mathbf{M}_s(e) \, \ddot{\mathbf{w}}_s^{(e)}, \tag{4.11}$$

where the matrix $\mathbf{M}_s^{(e)}$ is obtained from eq. (4.10) by sybstituting ρ_s to ρ_i (i = b, p);

$$\langle k \, w_s, \, \delta w_s \rangle = \sum_e \delta \mathbf{w}_s^{(e)T} \, \mathbf{K}_{sk}^{(e)} \, \mathbf{w}_s^{(e)}, \tag{4.12}$$

where:

$$\mathbf{K}_{sk}^{(e)} = \mathbf{k} \int_0^{\ell e} \mathbf{F}_w \, \mathbf{F}_w^T \, d\xi; \qquad \mathbf{K}_{sk}^{(e)} = 2\pi \, k \int_0^{\ell e} \mathbf{F}_w \, \mathbf{F}_w^T \, r \, d\xi; \tag{4.13}$$

$$\left\langle \frac{1}{\eta} (w_p - w_s)^+, \, \delta w_p - \delta w_s \right\rangle = \sum_e [\delta \mathbf{w}_p^{(e)T} \, \mathbf{H}_e \, \mathbf{w}_p^{(e)} + \delta \mathbf{w}_s^{(e)T} \, \mathbf{H}_e \, \mathbf{w}_s^{(e)} - \delta \mathbf{w}_p^{(e)T} \, \mathbf{H}_e \, \mathbf{w}_s^{(e)} - \delta \mathbf{w}_s^{(e)T} \, \mathbf{H}_e \, \mathbf{w}_p^{(e)}] \tag{4.14}$$

where we utilized a four points Gaussian quadrature formula:

$$\mathbf{H}_e = \frac{1}{\eta} \sum_{\gamma e} P_{\gamma e} \, \mathbf{F}_w \, (\xi_{\gamma e}) \, \mathbf{F}_w \, (\xi_{\gamma e}), \qquad \mathbf{H}_e = \frac{2\pi}{\eta} \sum_{\gamma e} P_{\gamma e} \, \mathbf{F}_w(\xi_{\gamma e}) \, \mathbf{F}_w^T(\xi_{\gamma e}) \, r(\xi_{\gamma e}), \tag{4.15}$$

and:

$$P_{\gamma e} = \begin{cases} 0 \text{ if } w_p(\xi_{\gamma e}) - w_s(\xi_{\gamma e}) < 0, \\ \text{Gaussian weight at the point } \xi_{\gamma e}; \end{cases} \tag{4.16}$$

$$\langle \tau, \, \delta u_p \rangle = \sum_e \left\{ \delta \mathbf{u}^{(e)T} \left[\mathbf{Q}_1^{(e)} \dot{\mathbf{u}}^{(e)} + \mathbf{Q}_2^{(e)} \, \dot{\mathbf{w}}'^{(e)} + \hat{\mathbf{Q}}_1^{(e)} \, \dot{\mathbf{u}}^{(e)} + \hat{\mathbf{Q}}_2 \, \dot{\mathbf{w}}'^{(e)} - \mathbf{q}_1^{(e)} \right] \right\}, \tag{4.17}$$

where:

$$\mathbf{Q}_1^{(e)} = \varepsilon_1 \sum_{\gamma e} P_{\gamma e} \, \mathbf{F}_u(\xi_{\gamma e}) \, \mathbf{F}_u^T(\xi_{\gamma e}), \qquad \mathbf{Q}_1^{(e)} = 2\pi\varepsilon_1 \sum_{\gamma e} P_{\gamma e} \, \mathbf{F}_u \, (\xi_{\gamma e}) \, \mathbf{F}_u^T(\xi_{\gamma e}) \, r(\xi_{\gamma e}), \tag{4.18}$$

$$\mathbf{Q}_2^{(e)} = \varepsilon_1 \frac{h}{2} \sum_{\gamma_e} P_{\gamma_e} \mathbf{F}_u(\xi_{\gamma_e}) \mathbf{F}_w'^{T}(\xi_{\gamma_e}),$$

$$\hat{\mathbf{Q}}_1^{(e)} = (\varepsilon_2 - \varepsilon_1) \sum_{\gamma_e} \hat{P}_{\gamma_e} \mathbf{F}_u(\xi_{\gamma_e}) \mathbf{F}_u^{T}(\xi_{\gamma_e}),$$

$$\hat{\mathbf{Q}}_2^{(e)} = (\varepsilon_2 - \varepsilon_1) \frac{h}{2} \sum_{\gamma_e} \hat{P}_{\gamma_e} \mathbf{F}_u(\xi_{\gamma_e}) \mathbf{F}_u'^{T}(\xi_{\gamma_e}),$$

$$\mathbf{q}_1^{(e)} = (\varepsilon_2 - \varepsilon_1) \sum_{\gamma_e} \phi_{\gamma_e} \hat{P}_{\gamma_e} \dot{\mathbf{u}}_0(\xi_{\gamma_e}) \mathbf{F}_u(\xi_{\gamma_e}),$$

$$\mathbf{Q}_2^{(e)} = 2\pi\varepsilon_1 \frac{h}{2} \sum_{\gamma_e} P_{\gamma_e} \mathbf{F}_u(\xi_{\gamma_e}) \mathbf{F}_w'^{T}(\xi_{\gamma_e}) r(\xi_{\gamma_e}), \quad (4.19)$$

$$\hat{\mathbf{Q}}_1^{(e)} = 2\pi(\varepsilon_2 - \varepsilon_1) \sum_{\gamma_e} \hat{P}_{\gamma_e} \mathbf{F}_u(\xi_{\gamma_e}) \mathbf{F}_u^{T}(\xi_{\gamma_e}) r(\xi_{\gamma_e}), \quad (4.20)$$

$$\hat{\mathbf{Q}}_2^{(e)} = 2\pi(\varepsilon_2 - \varepsilon_1) \frac{h}{2} \sum_{\gamma_e} \hat{P}_{\gamma_e} \mathbf{F}_u(\xi_{\gamma_e}) \mathbf{F}_u'^{T}(\xi_{\gamma_e}) r(\xi_{\gamma_e}), \quad (4.21)$$

$$\mathbf{q}_1^{(e)} = 2\pi(\varepsilon_2 - \varepsilon_1) \sum_{\gamma_e} \phi_{\gamma_e} \hat{P}_{\gamma_e} \dot{\mathbf{u}}_0(\xi_{\gamma_e}) \mathbf{F}_u(\xi_{\gamma_e}) r(\xi_{\gamma_e}), \quad (4.22)$$

being:

$$\hat{P}_{\gamma_e} = \begin{cases} 0 \quad \text{if } \left(| \dot{u}_p(\xi_{\gamma_e}) + \frac{h}{2} \dot{w}_p'(\xi_{\gamma_e}) | \; - \dot{u}_0(\xi_{\gamma_e}) \right) \leqslant 0 \\ P_{\gamma_e} = \text{Gaussian weight at the point } \xi_{\gamma_e} \end{cases} \quad (4.23a)$$

and:

$$\phi_{\gamma_e} = \begin{cases} 1 \quad \text{if } \dot{u}_p(\xi_{\gamma_e}) + \frac{h}{2} \dot{w}_p'(\xi_{\gamma_e}) \geqslant 0; \\ -1 \quad \text{if } \dot{u}_p(\xi_{\gamma_e}) + \frac{h}{2} \dot{w}_p'(\xi_{\gamma_e}) < 0; \end{cases} \quad (4.23b)$$

$$\left\langle \frac{h}{2} \sigma_r, \delta w_p' \right\rangle = \sum_e \left\{ \delta \mathbf{w}_p'^{T} \left[\mathbf{G}_1^{(e)} \dot{\mathbf{u}}^{(e)} + \mathbf{G}_2^{(e)} \dot{\mathbf{w}}'^{(e)} + \hat{\mathbf{G}}_1^{(e)} \dot{\mathbf{u}}^{(e)} + \hat{\mathbf{G}}_2^{(e)} \dot{\mathbf{w}}'^{(e)} - \mathbf{q}_2^{(e)} \right] \right\} \quad (4.24)$$

where:

$$\mathbf{G}_1^{(e)} = \varepsilon_1 \frac{h}{2} \sum_{\gamma_e} P_{\gamma_e} \mathbf{F}_w'(\xi_{\gamma_e}) \mathbf{F}_u^{T}(\xi_{\gamma_e}),$$

$$\mathbf{G}_2^{(e)} = \varepsilon_1 \frac{h^2}{4} \sum_{\gamma_e} P_{\gamma_e} \mathbf{F}_w'(\xi_{\gamma_e}) \mathbf{F}_u'^{T}(\xi_{\gamma_e}),$$

$$\mathbf{G}_1^{(e)} = (\varepsilon_2 - \varepsilon_1) \frac{h}{2} \sum_{\gamma_e} \hat{P}_{\gamma_e} \mathbf{F}_w'(\xi_{\gamma_e}) \mathbf{F}_u^{T}(\xi_{\gamma_e}),$$

$$\hat{\mathbf{G}}_2^{(e)} = (\varepsilon_2 - \varepsilon_1) \frac{h^2}{4} \sum_{\gamma_e} \hat{P}_{\gamma_e} \mathbf{F}_w'(\xi_{\gamma_e}) \mathbf{F}_w'^{T}(\xi_{\gamma_e})$$

$$\mathbf{q}_2^{(e)} = (\varepsilon_2 - \varepsilon_1) \frac{h}{2} \sum_{\gamma_e} \phi_{\gamma_e} \hat{P}_{\gamma_e} \dot{\mathbf{u}}_0(\xi_{\gamma_e}) \mathbf{F}_w'^{T}(\xi_{\gamma_e}),$$

$$\mathbf{G}_1^{(e)} = 2\pi\varepsilon_1 \frac{h}{2} \sum_{\gamma_e} P_{\gamma_e} \mathbf{F}_w'(\xi_{\gamma_e}) \mathbf{F}_u^{T}(\xi_{\gamma_e}) r(\xi_{\gamma_e}, \quad (4.25)$$

$$\mathbf{G}_2^{(e)} = 2\pi\varepsilon_1 \frac{h^2}{4} \sum_{\gamma_e} P_{\gamma_e} \mathbf{F}_w'(\xi_{\gamma_e}) \mathbf{F}_u'^{T}(\xi_{\gamma_e}) r\xi_{\gamma_e}), \quad (4.26)$$

$$\hat{\mathbf{G}}_1^{(e)} = 2\pi(\varepsilon_2 - \varepsilon_1) \frac{h}{2} \sum_{\gamma_e} \hat{P}_{\gamma_e} \mathbf{F}_w'(\xi_{\gamma_e}) \mathbf{F}_u^{T}(\xi_{\gamma_e}) r(\xi_{\gamma_e}), \quad (4.27)$$

$$\hat{\mathbf{G}}_2^{(e)} = 2\pi(\varepsilon_2 - \varepsilon_1) \frac{h^2}{4} \sum_{\gamma_e} \hat{P}_{\gamma_e} \mathbf{F}_w'(\xi_{\gamma_e}) \mathbf{F}_w'^{T}(\xi_{\gamma_e}) r(\xi\gamma_e), \quad (4.28)$$

$$\mathbf{q}_2^{(e)} = 2\pi(\varepsilon_2 - \varepsilon_1) \frac{h}{2} \sum_{\gamma_e} \phi_{\gamma_e} \hat{P}_{\gamma_e} \dot{\mathbf{u}}_0(\xi_{\gamma_e}) \mathbf{F}_w'^{T}(\xi\gamma_e) r(\xi_{\gamma_e}), \quad (4.29)$$

$\hat{P}_{\gamma_e}$, P_{γ_e} and ϕ_{γ_e} being defined by eqs. (4.23a) and (4.23b).

Let be now:

$$\mathbf{v}_e^* = \begin{bmatrix} \mathbf{u}_{(e)} \\ \mathbf{w}_i^{(e)} \\ \mathbf{w}_s^{(e)} \end{bmatrix} \quad (i = b, p) \quad (4.30)$$

$$\mathbf{K}_e^* = \left[\begin{array}{c|c|c} \mathbf{K}_u^{(e)} & \mathbf{0} & \mathbf{0} \\ \hline \mathbf{0} & \mathbf{K}_w^{(e)} & \mathbf{0} \\ \hline \mathbf{0} & \mathbf{0} & \mathbf{K}_s^{(e)} + \mathbf{K}_{sk}^{(e)} \end{array}\right], \tag{4.31}$$

$$\mathbf{M}_e^* = \left[\begin{array}{c|c|c} \mathbf{M}_u^{(e)} & \mathbf{0} & \mathbf{0} \\ \hline \mathbf{0} & \mathbf{M}_w^{(e)} & \mathbf{0} \\ \hline \mathbf{0} & \mathbf{0} & \mathbf{M}_s^{(e)} \end{array}\right], \tag{4.32}$$

$$\mathbf{H}_e^* = \left[\begin{array}{c|c|c} \mathbf{0} & \mathbf{0} & \mathbf{0} \\ \hline \mathbf{0} & \mathbf{H}_e & -\mathbf{H}_e \\ \hline \mathbf{0} & -\mathbf{H}_e & \mathbf{H}_e \end{array}\right], \tag{4.33}$$

$$\mathbf{C}_e^* = \sum_{i=1}^{2} \left[\begin{array}{c|c} \mathbf{Q}_i + \hat{\mathbf{Q}}_i + \mathbf{G}_i + \hat{\mathbf{G}}_i & \mathbf{0} \\ \hline \mathbf{0} & \mathbf{0} \end{array}\right], \tag{4.31}$$

Putting:

$$\bar{\mathbf{K}}_e^* = \mathbf{K}_e^* + \mathbf{H}_e^*, \tag{4.35}$$

the dynamical equilibrium equations (3.1) can be written in the form:

$$\sum_e \left\{ \mathbf{M}_e^* \ddot{\mathbf{v}}_e^* + \mathbf{C}_e^* \dot{\mathbf{v}}_e^* + \bar{\mathbf{K}}_e^* \mathbf{v}_e^* \right\} = \mathbf{q}_e^*, \tag{4.36}$$

where $\mathbf{q}_e^*$ represent the local load vector.

Introducing now the global quantities corresponding to the terms in eq. (4.36), we get the following finite element expression of eq. (3.1) [REDDY, 1984]:

$$\mathbf{M}\,\ddot{\mathbf{v}} + \mathbf{C}(\dot{\mathbf{v}}) + \mathbf{K}(\mathbf{v})\,\mathbf{v} = \mathbf{q}, \tag{4.37}$$

where $\mathbf{v}$ is the vector of nodal displacement, $\mathbf{M}$ is the mass matrix, $\mathbf{q}$ is the load vector, $\mathbf{K}(\mathbf{v})$ is the stiffness matrix and $\mathbf{C}(\dot{\mathbf{v}})$ is a damping matrix depending on the friction terms.

5. Solution algorithm

The solution of eq. (4.37) is obtained trough a semi-implicit integration method [GLOWINSKI *et al.*, 1976].

More precisely, the velocities and the accelerations are approximated by central finite differences and the solution at time $t + \Delta t$ is calculated by the dynamical equilibrium equations (4.37) relative to time t, assuming for the elastic force $\mathbf{K}(\mathbf{v})\,\mathbf{v}$ their value at time $t + \theta t$, where θ is a fixed number in [0, 1].

In more explicit terms, the step-by-step solution algorithm is the following:

$$\mathbf{v}_{t+\Delta t} = \hat{\mathbf{M}}^{-1}\,(\mathbf{v}_\theta,\ \dot{\mathbf{v}}_t)\ \hat{\mathbf{q}}(\mathbf{v}_\theta,\ \dot{\mathbf{v}}_t), \tag{5.1}$$

where:

$$\mathbf{v}_\theta = \mathbf{v}_t + \theta\,(\mathbf{v}_{t+\Delta t} - \mathbf{v}_t), \tag{5.2a}$$

$$\dot{\mathbf{v}}_t = \frac{1}{2\,\Delta t}\,(\mathbf{v}_{t+\Delta t} - \mathbf{v}_{t-\Delta t}), \tag{5.2b}$$

$$\hat{\mathbf{M}}\,(\mathbf{v}_\theta,\ \dot{\mathbf{v}}_t) = \frac{1}{\Delta t^2}\,\mathbf{M} + \theta\,\mathbf{K}(\mathbf{v}_\theta) + \frac{1}{2\,\Delta t}\,\mathbf{C}(\dot{\mathbf{v}}_t), \tag{5,2c}$$

$$\hat{\mathbf{q}}\,(\mathbf{v}_\theta,\ \mathbf{v}_t) = \mathbf{q}_t + \left[\frac{2}{\Delta t^2}\,\mathbf{M} + (\theta - 1)\,\mathbf{K}(\mathbf{v}_\theta)\right]\mathbf{v}_t - \left[\frac{1}{\Delta t^2}\,\mathbf{M} - \frac{1}{2\,\Delta t}\,\mathbf{C}(\dot{\mathbf{v}}_t)\right]\mathbf{v}_{t-\Delta t}. \tag{5.2d}$$

Eq. (4.38) is valid if $t>0$; in particular at time $t=0$ we put:

$$\mathbf{v}_{\Delta t} = \mathbf{v}_0 + \dot{\mathbf{v}}_0 \Delta t. \tag{5.3}$$

In order to calculate the non linear terms in eqs. (5.2c) and (5.2d), the following iterative procedure is employed:

$$\mathbf{v}^{(k)}_{t+\Delta t} = \hat{\mathbf{M}}^{-1}\,(\mathbf{v}^{(k-1)}_\theta,\ \dot{\mathbf{v}}^{(k-1)}_t)\ \hat{\mathbf{q}}(\mathbf{v}_\theta{}^{(k-1)},\ \dot{\mathbf{v}}^{(k-1)}_t), \tag{5.4}$$

being:

$$\mathbf{v}^{(k-1)}_\theta = \mathbf{v}_t + \theta\,(\mathbf{v}^{(k-1)}_{t+\Delta t} - \mathbf{v}_t), \tag{5.5a}$$

$$\dot{\mathbf{v}}^{(k-1)}_t = \frac{1}{2\,\Delta t}\,(\mathbf{v}^{(k-1)}_{t+\Delta t} - \mathbf{v}_{t-\Delta t}), \tag{5.5b}$$

6. Numerical results and conclusion

In this last section we give some numerical results relative to the load conditions shown in Fig. 6

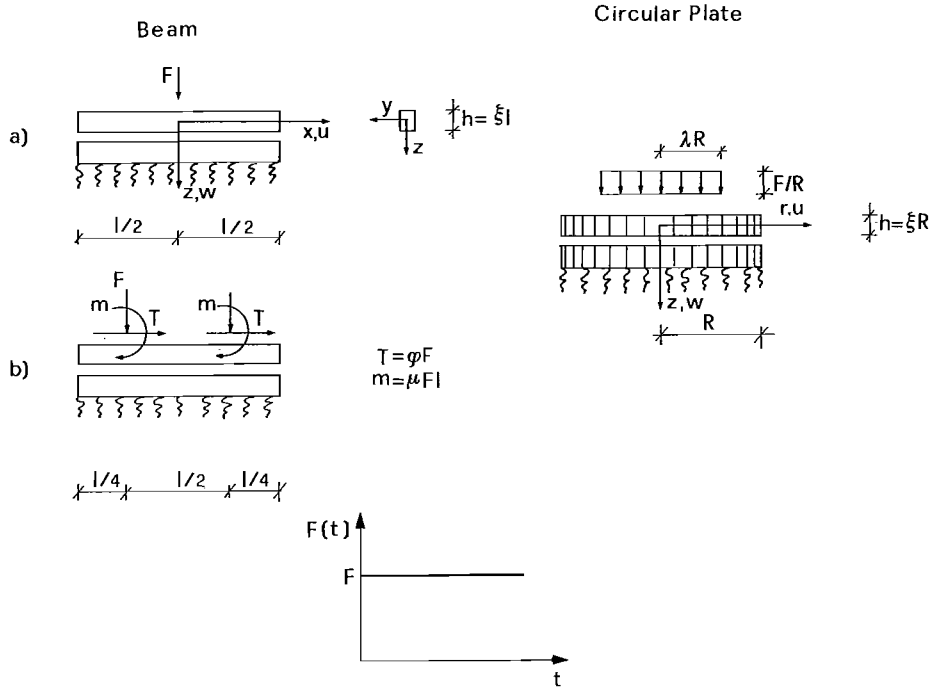

Fig. 6

In order to deal with dimensionless quantities we put:

Beam	Circular Plate	
$\zeta = x/\ell, \quad \zeta\in[-1/2,+1/2]$	$\zeta=r/R, \quad \zeta\in[0,1]$	(5.1a)
$W_i = w_i/\ell \quad (i=b,s)$	$W_i=w_i/R \quad (i=p,s),$	(6.1b)
$U_b = u_b/l,$	$U_p = u_p/R,$	(6.1c)
$\Sigma_x = \sigma_x l^3/D_b,$	$\Sigma_x = \sigma_x R^3/D_p,$	(6.1d)
$\Sigma_z = \sigma_z l^3/D_b,$	$\Sigma_z = \sigma_z R^3/D_p,$	(6.1e)
$\tau = t/T_0,$	$\tau = t/T_0,$	(6.1f)
where:	where:	
$T_0 = l^2(\rho_b/D_b)^{1/2}.$	$T_0 = R^2(\rho_p/D_p)^{1/2}.$	(6.1g)

Substituting eqs. (6.1) into eq. (3.1) it is easy to show that the solution of Problem A depends on the following dimensionless parameters:

$\xi = h/\ell,$	$\xi = h/R,$	(6.2a)
$\overline{\varepsilon_i} = \varepsilon_i l^2/(\rho_b D_b)^{1/2},$	$\overline{\varepsilon_i} = \varepsilon_i R^2/(\rho_r D_p^{1/2})$	(6.2b)
$\overline{\eta} = \eta D_b/l^4,$	$\overline{\eta} = \eta D_p/R^4,$	(6.2c)
$\alpha = D_s/D_b,$	$\alpha = D_s/D_p,$	(6.2d)
$\beta = kl^4/D_b,$	$\beta = k R^4/D_p,$	(6.2e)
$\gamma_b = C_b l^2/D_b,$	$\gamma_p = C_p l^2/D_p,$	(6.2f)
$\overline{\rho} = \rho_s/\rho_b,$	$\overline{\rho} = \rho_s/\rho_p,$	(6.2g)
f,	f, ν_p, ν_s,	(6.2h)
$\frac{Fl^2}{D_b}.$	$\frac{FR}{D_p}.$	(6.2i)

The following numerical results have been obtained by means of a uniform finite element mesh of $N_e=40$, 80, 100 elements. The local interpolants are linear polynomials for u_p and cubic Hermitian polynomials for w_i respectively.

In our numerical experiments we have assumed $\nu_p=\nu_s=0.2$, $\gamma_b=\gamma_p=1.2\times10^3$, $Fl^2/D_b=0.012$ and $FR/D_p=1.15$.

Further the initial conditions for displacements and velocities are assumed to be zero and the parameter θ in the semi-implicit scheme is taken to be 0.5.

The parameter $\overline{\varepsilon_2}$ is put equal to $1/\overline{\varepsilon_1}$.

6.1. Plate example

Firstly we examine the numerical convergence of the finite element model utilized.

Tab. 1 shows the value of the displacements U_p, W_p and W_s versus the dimensionless abscissa ζ for the three meshes characterized by $N_e=40$, 80, 100 elements.

Further tab. 2 shows the values found in the same cases for the interactions Σ_z and Σ_r.

Tabella 1

	NE = 40			NE = 80			NE = 100		
ζ	U_p	W_p	W_s	U_p	W_p	W_s	U_p	W_p	W_s
0.0	0.000E-0	0.128E-3	0.127E-3	0.000E-0	0.128E-3	0.127E-3	0.000E-0	0.128E-3	0.127E-3
0.2	−0.511E-6	0.894E-4	0.884E-4	−0.510E-6	0.894E-4	0.884E-4	−0.509E-6	0.894E-4	0.884E-4
0.4	−0.109E-5	0.187E-4	0.220E-4	−0.109E-5	0.187E-4	0.221E-4	−0.108E-5	0.187E-4	0.221E-4
0.6	−0.160E-5	−0.342E-4	0.114E-5	−0.160E-5	−0.342E-4	0.113E-5	−0.159E-5	−0.342E-4	0.114E-5
0.8	−0.194E-5	−0.492E-4	−0.178E-5	−0.194E-5	−0.492E-4	−0.178E-5	−0.193E-5	−0.492E-4	−0.178E-5
1.0	0.201E-5	0.431E-4	0.348E-6	0.201E-5	0.430E-4	0.347E-6	0.200E-5	0.430E-4	0.348E-6

$\alpha = 1.0$; $\beta = 1.0 \times 10^4$; $\overline{\eta} = 1.0 \times 10^{-6}$; $\overline{\rho} = 1.0$; $\overline{\varepsilon_1} = 1.0 \times 10^2$; $f = 0.5$

$\xi = 0.1$; $\lambda = 0.25$; $\tau = 0.14$; $\Delta\tau = 1.0 \times 10^{-3}$

Tabella 2

	NE = 40		NE = 80		NE = 100	
ζ	Σ_z	$\Sigma_r \times 10^3$	Σ_z	$\Sigma_r \times 10^3$	Σ_z	$\Sigma_r \times 10^3$
0.000	1.2106	0.0000	1.1206	0.0000	1.2106	0.0000
0.050	1.1984	−0.7602	1.1984	−0.7496	1.1984	−0.7621
0.100	1.1667	−1.5041	1.1667	−1.4895	1.1667	−1.4986
0.150	1.1172	−2.2375	1.1172	−2.2218	1.1173	−2.2384
0.200	0.9913	−3.1634	0.9913	−3.0616	0.9913	−3.0804
0.250	0.6869	−3.9268	0.6867	−3.6557	0.6869	−3.8740
0.300	0.4833	−2.3557	0.4831	−2.3052	0.4833	−2.3145

$\alpha = 1.0$; $\beta = 1.0 \times 10^4$; $\overline{\eta} = 1.0 \times 10^{-6}$; $\overline{\rho} = 1.0$; $\overline{\varepsilon_1} = 1.0 \times 10^2$; $f = 0.5$

$\xi = 0.1$; $\lambda = 0.25$; $\tau = 0.14$; $\Delta\tau = 1.0 \times 10^{-3}$

In particular Σ_z has been evaluted as $1/\eta\,(W_p - W_s)^+$. A plot of Σ_z versus the abscissa ζ is given by Fig. 7.

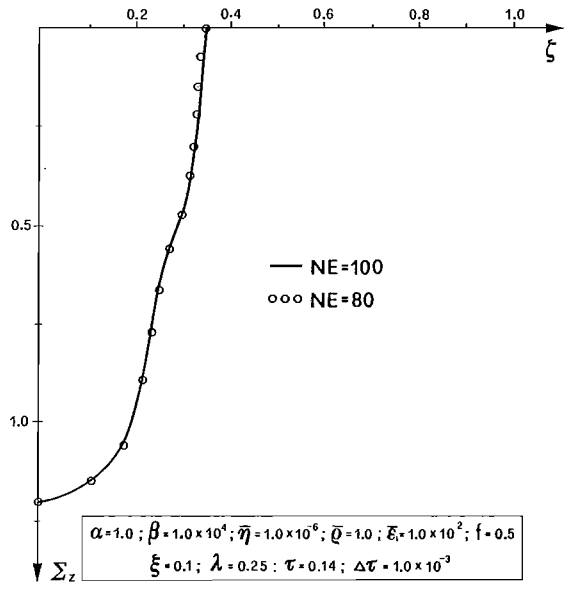

Fig. 7

We can observe that a good approximation is already obtained by using a mesh of 40 elements. The same behaviour has been observed in the beam example so that all the following results refer to such a finite element mesh.

The value $\overline{\eta} = 1.0 \times 10^{-6}$ utilized in the previous experiments is such that the numerical results are practically independent from this parameter.

The influence of the time stepsize $\Delta\tau$ has been also investigated. Tab. 3 shows the results of this analysis which enables us to assume in the following $\Delta\tau = 0.5 \times 10^{-3}$.

Tabella 3

	$\Delta\tau$ = 0.001		$\Delta\tau$ = 0.0005		$\Delta\tau$ = 0.0001	
τ	$\eta_p \times 10^4$	Σ_z	$W_p \times 10^4$	Σ_z	$W_p \times 10^4$	Σ_z
0.10	0.8032	0.97	0.8038	0.96	0.8027	0.96
0.11	1.0610	1.10	1.0690	1.10	1.0680	1.11
0.12	1.3080	1.21	1.3293	1.23	1.3700	1.27
0.13	1.4032	1.26	1.4400	1.28	1.4700	1.30
0.14	1.2836	1.21	1.3070	1.22	1.3300	1.24

$\alpha = 1.0$; $\beta = 1.0 \times 10^4$; $\overline{\eta} = 1.0 \times 10^{-6}$; $\overline{\rho} = 1.0$; $\overline{\varepsilon_1} = 1.0 \times 10^2$; $f = 0.5$
$\xi = 0.1$; $\lambda = 0.25$

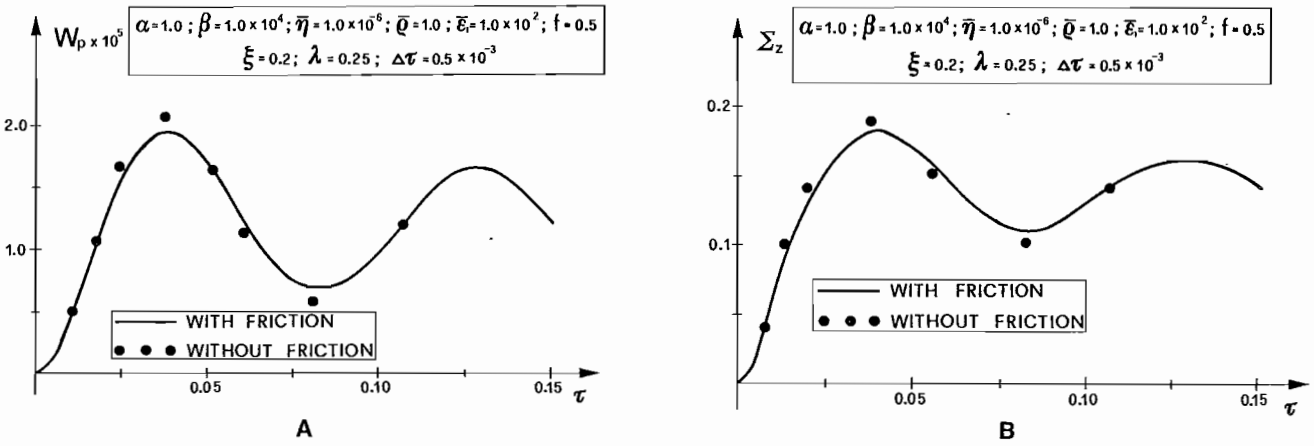

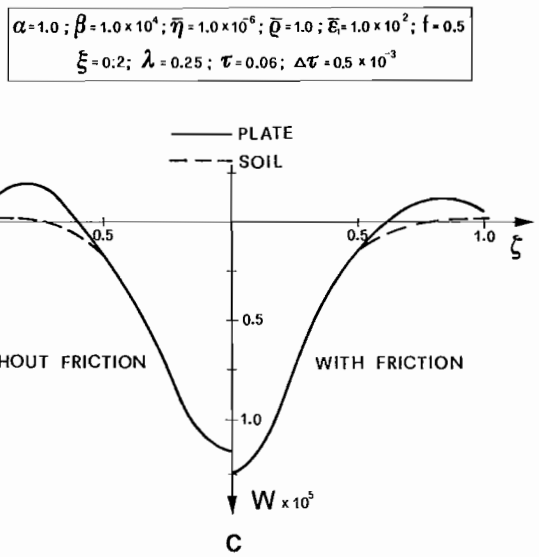

Fig. 8

Another kind of analysis developed concerns the influence of the parameter ξ which is relative to the work done by the tangential stresses Σ_r. As Figs.9 show this influence can be significant.

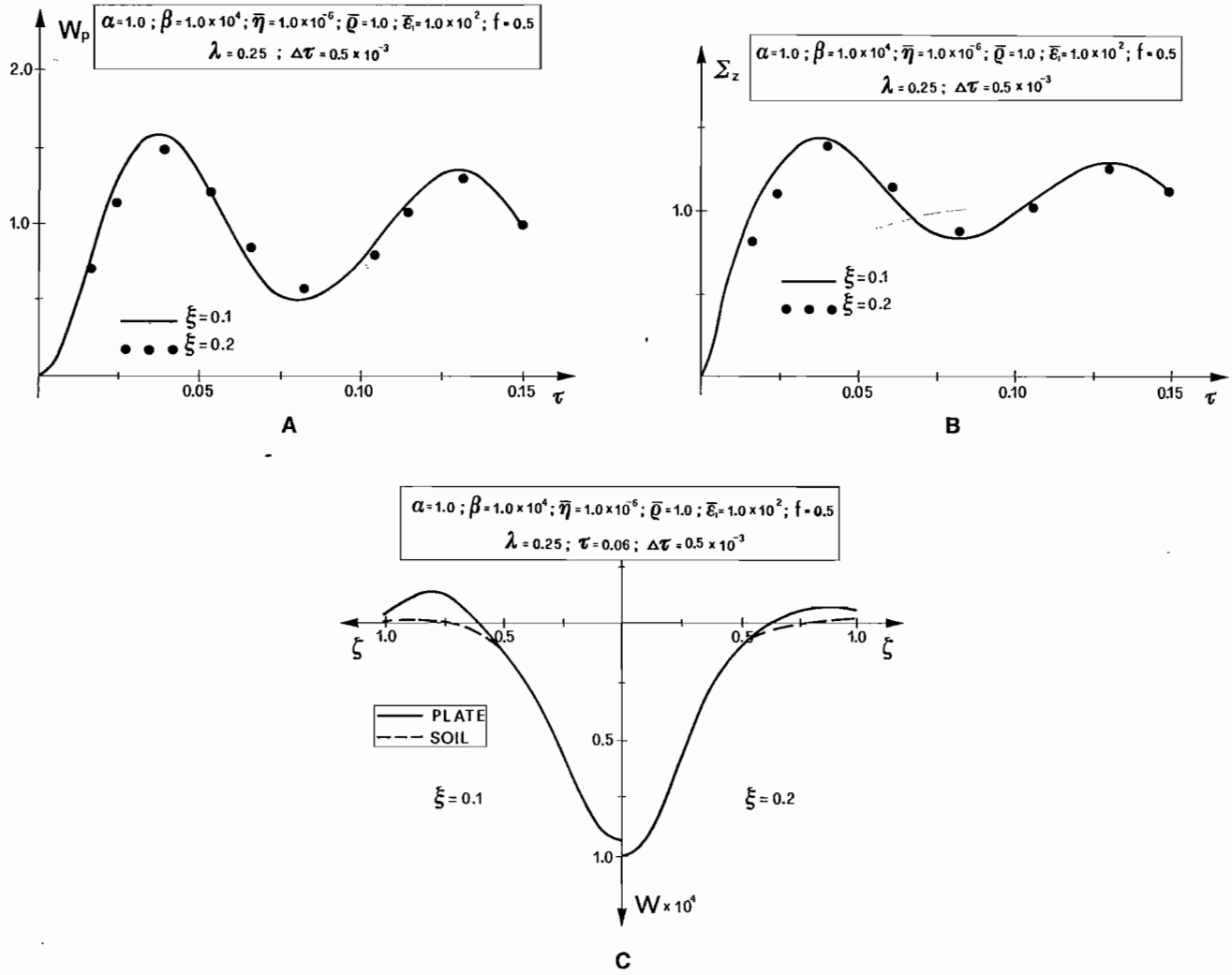

Fig. 9

The influence of the mass density ratio $\overline{\rho} = \rho_s/\rho_p$ has also been investigated: in particular the case $\overline{\rho} = 1$ and $\overline{\rho} = 0$ have been analysed. The corresponding results are summarized in Figs. 10.

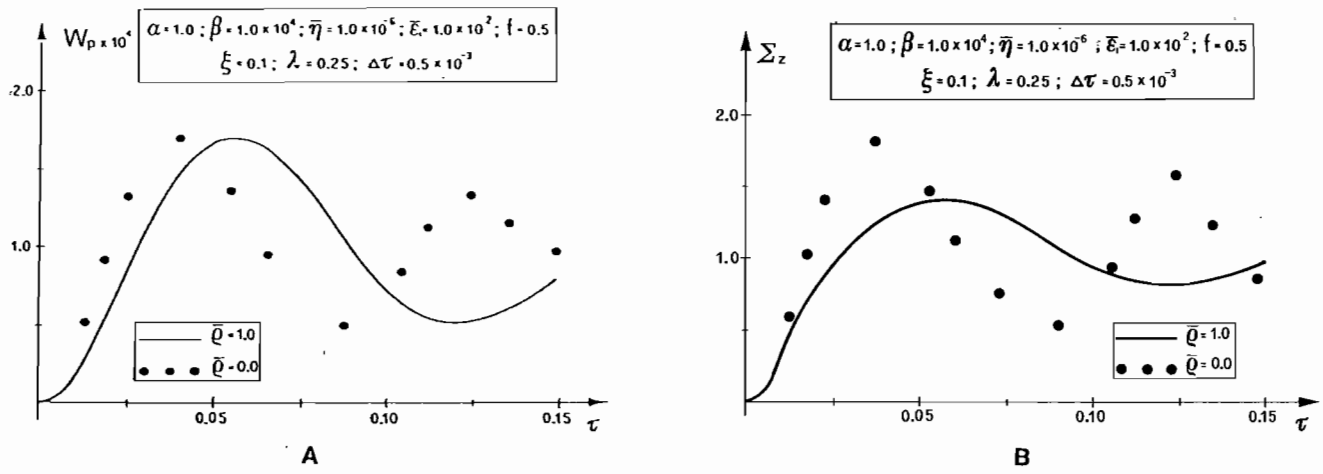

Fig. 10

6.2 *Beam example*

For that it concerns the beam example, we assume the following values of the dimensionless parameters:

$$\overline{\varepsilon_1} = 1.0 \times 10^2,\ \overline{\varepsilon_2} = 1.0 \times 10^{-2},\ \overline{\eta} = 1.0 \times 10^{-10}, \quad (6.3a)$$

$$\alpha = 1.0,\ \overline{\rho} = 1.0,\ \xi = 0.2 \quad (6.3b)$$

$$\gamma = 1.0 \times 10^3,\ f = 0.8,\ \frac{Fl^2}{D_b} = 0.012 \quad (6.3c)$$

With reference to these value, Figs. 11a-11b show the plots of the lateral deflection along the beam axis for an assigned time $\tau = 0.30$. The first one refers to the load condition a), while the second refers to the load condition b) ($\varphi = 0.1$, $\mu = 0.2$).

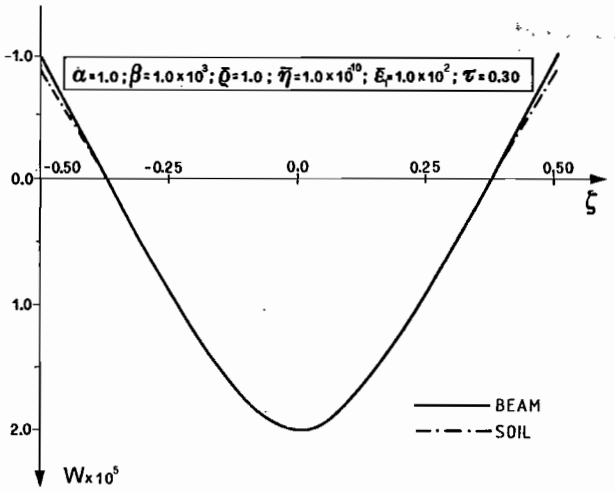

A

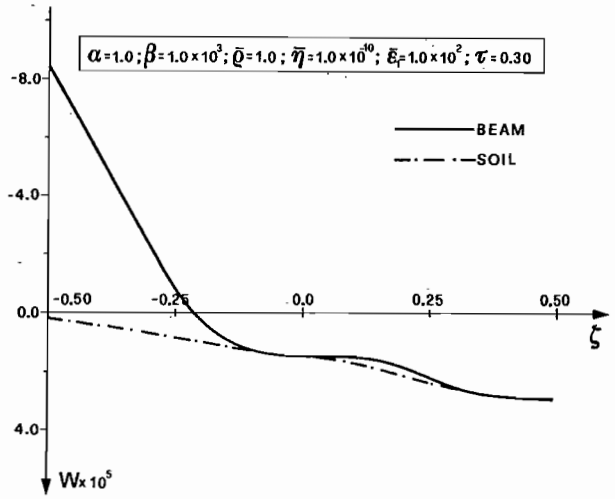

B

Fig. 11

The same figures show how the load condition can modify the contact region between structures and foundation. In fact, for the same values of the stiffness parameter α and β, we observe that the contact is almost complete under the load condition a), while the unbonding area becomes relevant in the presence of moments and horizontal loads. This observation is of great significance when analyzing interaction forces under seismic loads.

The dependence on the time for displacements is analysed in Figs 12a-12b.

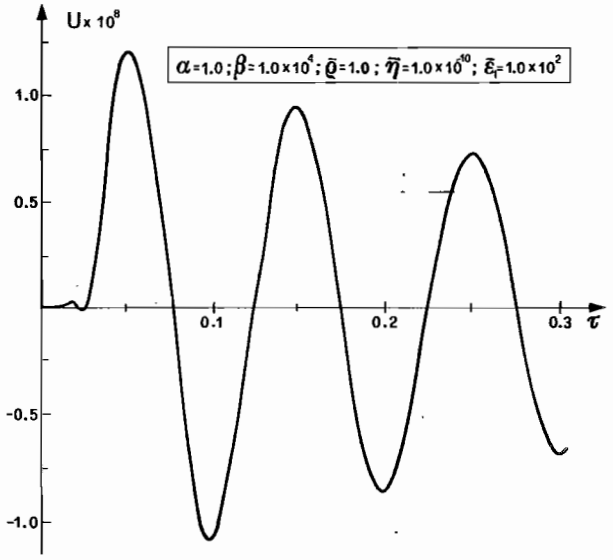

A

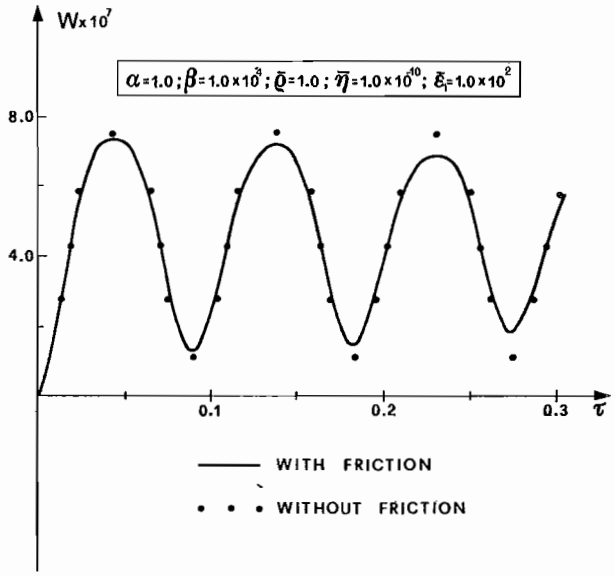

B

Fig. 12

In particular, these figures show the plots of the vertical and horizontal displacements shown by the beam central and end cross section, respectively (load condition a)).

It is evident that the damping effect is due to the

presence of the friction forces. Finally Figs. 13a-13b give a comparison between the beam lateral deflections (load condition a)) with or without friction.

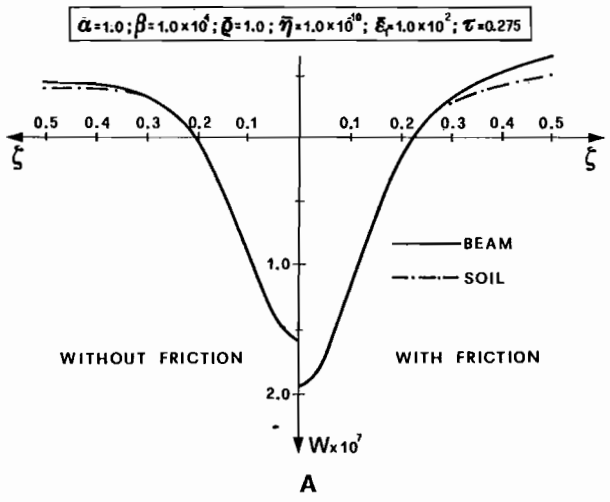

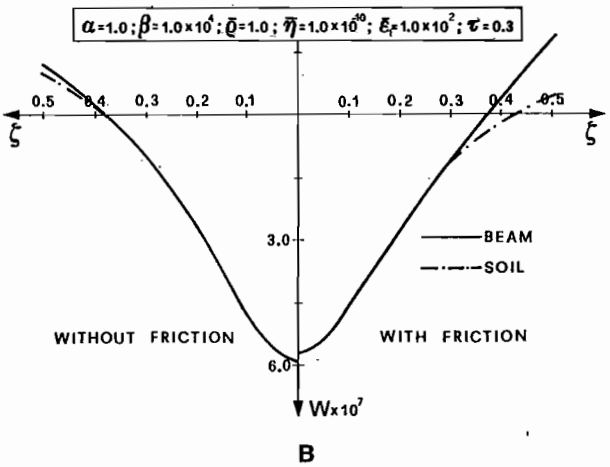

Fig. 13

We observe that the friction can modify not only the contact area but also the value of the maximum lateral deflection. In particular, in our case we found differences greater than 20%.

BIBLIOGRAFIA

ASCIONE L., BRUNO D., OLIVITO R.S. (1984) - *On the Dynamical Behaviour of Plates in Unilateral Contact with an Elastic Foundation: A Finite Element Approach*. Atti dell'Accademia Nazionale dei Lincei, Vol. LXXVI, fasc. 1, gennaio.

ASCIONE L., BRUNO D. (1984) - *Sul Problema Dinamico di Contatto Monolaterale fra Piastre e Fondazioni*. Proc. of the 8-th National Congress AIMETA, 2, 637-641.

ASCIONE L., BILOTTI G. (1989) - *The Dynamical Problem of an Elastic Plate Resting on a Tensionless Two-parameter Foundation*. To appear on MECCANICA.

ASCIONE L., BRUNO D. (1984) - *The Unilateral Contact Problem with Friction of a Plate Resting on an Elastic Half-Space*. Rep. n. 71, Dept. of Structures, Univ. of Calabria.

BILOTTI G., OLIVITO R.S. (1986) - *A Numerical Investigation on the Unilateral Contact Problem with Friction*. Rivista Italiana di Geotecnica, vol. 3, 135-148.

DUVAUT G., LIONS J.L. (1980) - *Les Inéquations en Mécanique et en Physique*. Dunod-Paris.

GLADWELL G.M.L. (1980) - *Contact Problems in the Theory of Elasticity*. Sijthoff & Noordhoff.

GLOWINSKI R., LIONS J.L., TRÈMOLIÈRES R. (1976) - *Analyse Numérique des Inéquations Variationnelles*. Dunod-Paris.

MITSOPOULOU E. (1983) - *Unilateral Contact, Dynamic Analysis of Beams by a Timestepping, Quadratic Programming Procedure*. Meccanica, 18, 254-265.

PANAGIOTOPOULOS P.D., TALASLIDIS D. (1980) - *A Linear Analysis Approach to the Solution of Certain Classes of Variational Inequality Problems in Structural Analysis*. Int. J. Solids Struct., 16, 991-1005.

REDDY J.N. (1984) - *An Introduction to the Finite Element Method*, McGraw-Hill Book Company.

SELVADURAI A.P.S. (1976) - *Elastic Analysis of Soil - Foundation Interaction*. Elsevier Scientific Publishing Company.

TOSCANO R. (1983) - *Un Problema Dinamico per la Piastra su Suolo Elastico Unilaterale*. Proc. of the second meeting on Unilateral Problems in Structural Analsys, (Editors: G. Del Piero and F. Maceri), Ravello, september 22-24.

SOMMARIO

Un'analisi del problema di contatto dinamico monolaterale con attrito di travi e piastre su fondazioni alla Hetényi

L'ipotesi di contatto monolaterale tra struttura di fondazione e terreno assume un importante significato in tutti quei problemi nei quali l'area di contatto tende a ridursi per motivi legati sia al carico, sia alla rigidezza relativa suolo-struttura.

Le diverse ricerche sviluppate in questo campo riguardano essenzialmente il caso statico [DUVAUT, LIONS, 1980; GLADWELL, 1980]. Meno investigato risulta invece il problema di interazione dinamica con vincolo monolaterale [PANAGIOTOPOULOS, TALASLIDIS, 1980; MITSOPOULOU, 1983; TOSCANO, 1983, ASCIONE *et al.*, 1984]. Tale problema presenta infatti difficoltà analitiche ben più ponderose del corrispondente problema statico.

Alcuni vantaggi analitici possono essere conseguiti utilizzando modelli semplificati di suolo, che permettono di cogliere gli aspetti numerici più significativi del problema senza eccessive difficoltà. Un'ampia rassegna di modelli di questo tipo è contenuta nel testo di SELVADURAI [1976].

Tra questi un giusto compromesso tra semplicità e bontà della schematizzazione introdotta è rappresentato dal modello di Hetényi.

In alcuni precedenti lavori [ASCIONE *et al.*, 1986; ASCIONE, BILOTTI, 1989], tale modello è stato utilizzato per analizzare l'interazione dinamica suolo-struttura nel caso di modelli monodimensionali di travi e piastre circolari assialsimmetriche in assenza di attrito.

In questo lavoro l'analisi viene integrata tenendo conto dell'effetto delle tensioni tangenziali generate dall'attrito, che insorge all'interfaccia tra suolo e struttura.

La legge di attrito ipotizzata è illustrata in Fig. 2, dove τ rappresenta la tensione tangenziale agente sul terreno e $\dot{\delta}$ è la velocità relativa orizzontale tra struttura di fondazione e terreno: sia τ che $\dot{\delta}$ sono evidentemente valori locali, variabili da punto a punto della fondazione.

Tale legge può essere interpretata come una regolarizzazione della classica legge di attrito dinamico di Coulomb, alla quale tende per $\varepsilon_1 \to \infty$ e $\varepsilon_2 \to 0$.

Il problema di contatto dinamico esaminato (Fig. 1) è riconducibile all'equazione (2.6) (*Problema P*).

In particolare le equazioni (2.6a-b) corrispondono rispettivamente

alle formulazioni variazionali (principio dei lavori virtuali) delle equazioni del moto della trave (o della piastra) e della sottostante fondazione alla Hetényi (quest'ultima supposta inestensibile).

Le equazioni (2.6c-d-e) caratterizzano invece l'interazione di tipo monolaterale tra suolo e struttura.

Le equazioni (2.6) sono evidentemente non lineari sia per la presenza del vincolo $\sigma_2 > 0$, legato all'ipotesi di incapacità del terreno a resistere a sforzi di trazione, sia per la presenza nella (2.6a) del termine del lavoro corrispondente alle forze di attrito la cui legge (2.3) è non lineare.

Allo scopo di superare le difficoltà matematiche connesse alla presenza delle disequazioni (2.6c) e (2.6d), riesce utile riferirsi ad un problema ausiliario ottenuto dal *Problema P* modificando opportunamente le condizioni di contatto.

Più precisamente (Fig. 4) si suppone che il generico punto della piastra π_p (struttura di fondazione) possa subire uno spostamento trasversale maggiore del corrispondente punto appartenente alla piastra π_s (suolo alla Hetényi). Nei punti in cui ciò si verifica si attivano delle molle di richiamo di rigidezza $1/\eta$, che tendono ad opporsi alla compenetrazione delle due piastre. È facile intuire che al tendere di $\eta \to 0$, cioè quando la rigidezza delle molle cresce indefinitamente, il problema ausiliario 'tende' al *Problema P*.

Da un punto di vista matematico, la formulazione del problema ausiliario (*Problema A*) è rappresentata dalla equazione variazionale (3.1). Si osserva che tale equazione è non lineare per la presenza del lavoro delle molle di richiamo e delle tensioni tangenziali agenti all'interfaccia terreno-struttura.

La forma esplicita di tutti i termini dell'eq. (3.1), relativamente ai due casi esaminati in Fig. 3a e 3b, è riportata nelle formule (3.2)-(3.11).

Il *Problema A* viene affrontato in questo lavoro dal punto di vista numerico mediante discretizzazione agli elementi finiti.

Utilizzando le interpolazioni (4.1a-b) è facile pervenire mediante passaggi standard, alla equazione (4,37), che rappresenta la versione discretizzata della (3.1). In essa $\ddot{\mathbf{v}}$ è il vettore degli spostamenti nodali, **M** è la matrice delle masse, q il vettore dei carichi, **K(v)** è la matrice delle rigidezze e **C(v)** è una matrice di tipo viscoso, legata ai termini di attrito.

L'integrazione nel tempo dell'eq. (4.37) è stata ottenuta mediante un metodo di tipo semi implicito [Głowinski *et al.*, 1976]. Più precisamente la velocità e l'accelerazione sono approssimate mediante differenze finite di tipo centrale e la soluzione al tempo $t + \Delta t$ è ottenuta dall'equazione di equilibrio dinamico (4.37) scritta al tempo t, assumendo per le forze elastiche **K(v)** la determinazione che ad esse compete all'istante $t + \theta\ \Delta t$, essendo θ un numero reale fissato nell'intervallo (0, 1).

Per quanto concerne l'esempio piastra (Fig. 6), è stata svolta innanzitutto un'indagine sulla convergenza del modello numerico agli elementi finiti, che utilizza per gli spostamenti assiali U_p una approssimazione lineare e per gli spostamenti trasversali W_p e W_s un'approssimazione cubica di tipo hermitiano.

I risultati di questa indagine sono sintetizzati nelle tabelle 1 e 2, dove sono contenuti i valori degli spostamenti U_p, W_p, W_s ed i valori delle interazioni normali e tangenziali Σ_z e Σ_r corrispondenti a mesh uniformi di 40, 80 e 100 elementi finiti.

L'esame di tali risultati porta a concludere che una buona approssimazione della soluzione è ottenuta già per una mesh di 40 elementi.

L'influenza sulla soluzione dell'intervallo di integrazione $\Delta\tau$ è illustrato nella tabella 3 ed i risultati conseguiti giustificano la scelta del valore $\Delta\tau = 0.5 \times 10^{+3}$, utilizzato nell'indagine numerica svolta.

La Fig. 8 istituisce un confronto tra il caso con attrito ($f = 0.5$) e quello senza attrito. In particolare le Figg. 8a-b mostrano l'andamento nel tempo dello spostamento W_p e della pressione Σ_Z esibiti dal punto centrale della piastra. La Fig. 8c mostra invece la deformata della piastra e del suolo lungo il raggio per un prefissato istante di tempo ($\tau = 0.06$).

L'influenza del parametro h/R, legato al lavoro compiuto dalle tensioni tangenziali da attrito Σ_r, è evidenziata nelle Figg. 9a-c dalle quali è possibile dedurre che tale parametro può modificare in maniera significativa la soluzione.

Infine, nella Fig. 10, si pongono a confronto le risposte strutturali nei due casi di suolo con massa ($\rho_s/\rho_p = 1$) e suolo senza massa ($\rho_s/\rho_p = 0$).

Per quanto riguarda l'esempio trave, un primo confronto è istituito tra le due condizioni di carico indicate nelle Figg. 6a-b. I risultati dell'indagine sono evidenziati dai grafici delle Figg. 11-a-b, che si riferiscono alla deformata della trave e del sottostante terreno ad un assegnato istante $\tau = 0.3$. Dal confronto si deduce come la condizione di carico possa modificare sensibilmente la zona di contatto, che si riduce vistosamente in presenza di forze orizzontali. Tale considerazione assume un importante significato se si pensa all'interesse tecnico presentato dallo studio dell'interazione suolo-struttura sotto carichi sismici.

L'influenza dell'attrito è indagata nelle Figg. 13a-b: si osserva come tale fenomeno possa modificare non solo l'area di contatto ma anche il valore della massima deflessione, con uno scostamento che nel caso esaminato è dell'ordine del 20%.